

Electronic Determinants of Photoacidity in Cyanonaphthols

Noam Agmon,^{*,†} Wolfgang Rettig,[‡] and Christian Groth[‡]*Contribution from the Department of Physical Chemistry, The Hebrew University, Jerusalem 91904, Israel, and the Institute of Chemistry, Humboldt-University of Berlin, Bunsenstrasse 1, D-10117 Berlin, Germany*

Received November 6, 2000

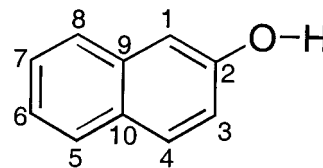
Abstract: We present semiempirical AM1 calculations for the ground and excited state of 2-naphthol and some of its cyano derivatives in the gas phase. Following photoexcitation, the Mulliken electron density on the oxygen diminishes slightly for the acid and more conspicuously for the anionic conjugated base. This agrees with the measured solvatochromic parameters for 2-naphthol. In both electronic states, we find a nice correlation with the measured pK values in water. The electronic charge distribution on the distal ring of the anion agrees with the experimental acidity order in both S_0 and S_1 . Upon excitation, it increases predominantly in positions 3, 5, and 8. The ring system of the anion assumes an alternant quinoidal structure in the ground state of the anion, which becomes more symmetric in the relaxed excited state. This suggests that the enhanced aromatic character of a 4n electron system in the excited state allows for better delocalization of the oxygen charge within the ring.

Introduction

Hydroxyaryls become strong acids in their excited singlet state (S_1).^{1,2} For example, the pK of 2-naphthol (2OH, Chart 1) in its ground state is 9.5, dropping to $pK^* = 2.8$ in S_1 , nearly 7 orders of magnitude. A common explanation for this effect is intramolecular charge transfer (ICT), in the excited state (ES) of the acid, from the hydroxyl oxygen to the aromatic ring.^{3–7} It was subsequently realized that the ICT effect must be even larger in the conjugate anionic base.⁸ Indeed, recent solvatochromic studies of 2OH have shown⁹ that although the effect exists in the acid form (ROH), it is considerably larger for the base (RO^-). Section II gives a detailed survey of experimental studies corroborating this observation. Thus, it is the *excess stabilization* of the excited anionic base that renders the ES deprotonation reaction more exothermic, leading to enhanced photoacidity.

This modified ICT ansatz has recently been confirmed theoretically by Granucci et al.,¹⁰ who have performed extensive ab initio calculations on phenol and cyanophenols. They observed that the dipole moment of phenol varies only slightly between S_0 and S_1 for the acid form but much more dramatically for the base. However, the dipole moment presents only an

Chart 1. Structure of 2-Naphthol (2OH) with Its Conventional Numbering Scheme



average measure for the charge density distribution, and moreover, for ions it depends on an arbitrary choice of the origin. To monitor the charge migration from the oxygen atom, it is preferable to consider the Mulliken charge on this atom,⁵ as well as the CO bond length. These attributes are probed below using semiempirical (AM1) calculations for 2OH and its cyano derivatives.

The confirmation of the dominance of electronic effects on the anionic product of ES proton dissociation by itself offers no explanation for the origin of the enhanced acidity of these excited aromatic dyes. The question that arises is, what produces the enhanced ICT in the excited RO^- ? According to the avoided crossing scenario,^{8,10–12} in phenol and 1-naphthol (1OH), the first two singlet levels interchange upon protonation: S_2 is more polar than S_1 in ROH, and it becomes the S_1 state of RO^- . It is, however, doubtful whether this provides a general criterion for the relative stability of the excited anion. The $S_1 - S_2$ avoided crossing does not seem to occur in 2OH,^{8,13} and in its cyano derivatives investigated below, although the latter are more acidic than 1OH. In 1OH, it occurs in the more polar solvents, but this is not sufficient for promoting ES proton transfer (PT).¹³ Despite the level crossing in 1OH, its excited

[†] The Hebrew University.

[‡] Humboldt-University of Berlin.

- (1) Förster, T. *Z. Elektrochem.* **1950**, *54*, 531.
- (2) Weller, A. *Prog. React. Kinet.* **1961**, *1*, 187.
- (3) Weller, A. *Z. Elektrochem.* **1952**, *56*, 662.
- (4) Jackson, G.; Porter, G. *Proc. R. Soc., London A* **1961**, *260*, 13.
- (5) Baba, H.; Suzuki, S. *J. Chem. Phys.* **1961**, *35*, 1118.
- (6) Kimura, K.; Tsubomura, H. *Mol. Phys.* **1966**, *11*, 349.
- (7) Mataga, N.; Kubota, T. *Molecular Interactions and Electronic Spectra*; Marcel Dekker: New York, 1970.
- (8) Schulman, S. G. *Spectrosc. Lett.* **1973**, *6*, 197.
- (9) Solntsev, K. M.; Huppert, D.; Agmon, N. *J. Phys. Chem. A* **1998**, *102*, 9599.
- (10) Granucci, G.; Hynes, J. T.; Millié, P.; Tran-Thi, T.-H. *J. Am. Chem. Soc.* **2000**, *122*, 12243.

(11) Webb, S. P.; Philips, L. A.; Yeh, S. W.; Tolbert, L. M.; Clark, J. H. *J. Phys. Chem.* **1986**, *90*, 5154.

(12) Knochenmuss, R.; Leutwyler, S. *J. Chem. Phys.* **1989**, *91*, 1268.

(13) Magnes, B.-Z.; Strashnikova, N. V.; Pines, E. *Isr. J. Chem.* **1999**, *39*, 361.

(neutral) methoxy derivative does appear to undergo pronounced ICT.^{14,15} Finally, for substituted naphthols, the distinction between the two excited singlet states (in terms of polarity and transition-dipole direction) becomes blurred altogether.

Since the common denominator of these photoacids is their aromaticity, one wonders why this factor has not been considered in more detail. To investigate possible connections with the concept of aromaticity,¹⁶ we extend our charge density and geometry calculations to the aromatic ring system of the 2OH molecule. We find indications that the excited base stabilization is connected with the inversion of the aromatic/antiaromatic character in the ES.^{17–20} In addition, we investigate the connection between the charge density, ionic resonance structures, and substituent effects at specific ring sites.

The substituent effect provides an additional probe for the ICT ansatz, since electron-withdrawing substituents (such as the CN group) are expected to further assist in charge migration, thus enhancing the photoacidity.^{21–23} Indeed we find (section IV) nice correlations between the calculated charge on the hydroxyl oxygen (and the CO bond length) with the measured pK values of cyano-2-naphthols in *both* electronic states. Such correlations have previously been attempted for amino aromatics,^{24–28} mainly in the ground state, and it was usually possible to obtain a good correlation only with some complex functional of the charge density.

The insight gained from these various probes may hopefully lead to better understanding of photoacidity and serve as a useful guide for future synthetic work.

Experimental Evidence of ICT

Several experimental findings indicate that ICT occurs for both excited acid and anion and that the effect on the anion is larger. If excitation causes charge migration to the distal ring, as is commonly believed,^{21–23} electron-withdrawing substituents on this ring should make ES proton dissociation even more exothermic, lowering the pK*. Indeed, the pK* value of the cyano-substituted 2-naphthols²³ drops to around -0.5 and that of a dicyano derivative to ~ -4 (see Table 1). This decrease is significantly greater than the decrease in ground-state pK values, reflecting the greater importance of the ICT contribution in the ES of the anion.²¹

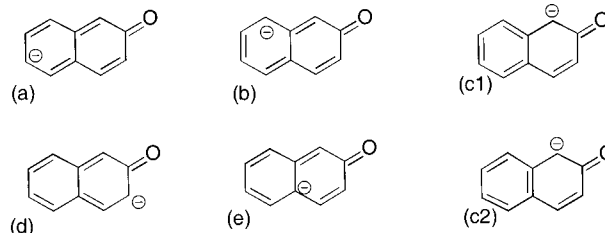
Chart 2 shows the five resonance structures for 2-naphtholate, in which the negative charge may reside on every second ring carbon atom (starting with C₂). Structures a and b suggest that, in the distal ring, the charge migrates to positions 6 and 8. Commensurate with this observation, we find (Table I) that the

Table 1. Experimental Values^{21–23} for Ground- and Excited-State pK Values of Cyano-Substituted 2-Naphthols in Water^a

molecule	pK	pK*
2OH	9.5	2.8
5CN	8.75	-0.75
6CN	8.4	-0.4
7CN	8.75	-0.2
8CN	8.35	-0.75
5,8DCN	7.8	-4.5

^a Errors in GS pK values are estimated at ± 0.1 whereas for ES pK* values they can be ± 0.5 pK unit. The increased uncertainty in the ES values is due to ES relaxation not accounted for in the Förster cycle and differences between these steady-state and dynamic pK estimates.

Chart 2. Ionic Resonance Structures for 2-Naphtholate



ground-state (GS) pK values of the 6- and 8-derivatives are lower than those for the 5- and 7-substitution. In the ES, however, it appears that 5- and 8-derivatives are the most acidic among the monosubstituted 2OH derivatives.²³ We are not aware of any role attributed, according to the literature, to structures c–e.

In 1-naphthol, position 5 seems to be the most active in the ES. For 1-methoxynaphthalene (1OMe), in which no proton dissociation can occur, NMR studies¹⁴ show greatly enhanced photochemical H/D exchange at position 5. In comparison, thermal (348 K) H/D exchange occurs mainly at position 2. Proton electrophilic attack on C₅ was also implicated in promoting ES fluorescence quenching in 1OMe.¹⁵ This experimental evidence suggests that ICT in 1OH occurs already in the excited acid.

The ICT ansatz helps to rationalize the spectral shifts of 2OH derivatives.^{5,9,29–31} Cyano substituents on the distal ring shift the fluorescence emission to the red by withdrawing excess electronic charge. ROH solvatochromic shifts are controlled by dipolar and hydrogen bond (HB) accepting properties of the solvent (the Kamlet–Taft³² π^* and β parameters, respectively). Concomitant with the ICT ansatz, the HB to the solvent **S**, ROH \cdots **S**, becomes stronger in S₁, leading to a larger sensitivity to β in the emission spectra as compared with the absorption (or excitation) spectra.^{29,30}

The ICT effect plays a larger role in stabilizing the anion (naphtholate base), where a full negative charge on the oxygen needs to be dispersed.⁸ Protic solvents (HS) can further assist by HB formation, RO⁻ \cdots HS. Indeed, solvatochromic shifts for 2-naphtholate correlate exclusively with the Kamlet–Taft α parameter describing the HB-donating properties of the solvent.⁹

- (14) Tobita, S.; Shizuka, H. *Chem. Phys. Lett.* **1980**, *75*, 140.
 (15) Shizuka, H. *Acc. Chem. Res.* **1985**, *18*, 141.
 (16) Minkin, V. I.; Glukhovtsev, M. N.; Simkin, B. Y. *Aromaticity and Antiaromaticity. Electronic and Structural Aspects*; Wiley: New York, 1994.
 (17) Baird, N. C. *J. Am. Chem. Soc.* **1972**, *94*, 4941.
 (18) Zilberg, S.; Haas, Y. *J. Phys. Chem. A* **1998**, *102*, 10843.
 (19) Shaik, S.; Shurki, A.; Danovich, D.; Hiberty, P. C. *Chem. Rev.* **2001**, *101*, 1501.
 (20) Wiberg, K. B. *Chem. Rev.* **2001**, *101*, 1317.
 (21) Tolbert, L. M.; Haubrich, J. E. *J. Am. Chem. Soc.* **1990**, *112*, 8163.
 (22) Tolbert, L. M.; Haubrich, J. E. *J. Am. Chem. Soc.* **1994**, *116*, 10593.
 (23) Huppert, D.; Tolbert, L. M.; Linares-Samaniego, S. *J. Phys. Chem. A* **1997**, *101*, 4602.
 (24) Grabowska, A.; Pakula, B.; Pancif, J. *Photochem. Photobiol.* **1969**, *10*, 415.
 (25) Waluk, J.; Grabowska, A.; Lipinski, J. *Chem. Phys. Lett.* **1980**, *70*, 175.
 (26) Spanget-Larsen, J. *J. Chem. Soc., Perkin Trans. 2* **1985**, 417.
 (27) Waluk, J.; Rettig, W.; Spanget-Larsen, J. *J. Phys. Chem.* **1988**, *92*, 6930.
 (28) Spanget-Larsen, J. *J. Phys. Org. Chem.* **1995**, *8*, 496.

- (29) Solntsev, K. M.; Huppert, D.; Tolbert, L. M.; Agmon, N. *J. Am. Chem. Soc.* **1998**, *120*, 7981.
 (30) Solntsev, K. M.; Huppert, D.; Agmon, N. *J. Phys. Chem. A* **1999**, *103*, 6984.
 (31) Solntsev, K. M.; Huppert, D.; Agmon, N.; Tolbert, L. M. *J. Phys. Chem. A* **2000**, *104*, 4658.
 (32) Kamlet, M. J.; Abboud, J.-L. M.; Abraham, M. H.; Taft, R. W. *J. Org. Chem.* **1983**, *48*, 2877.

Table 2. Calculated (AM1, 16 CI Orbitals) $S_0 \rightarrow S_1$ (ΔE_1), $S_0 \rightarrow S_2$ (ΔE_2), $S_1 \rightarrow S_0$ (ΔE_{-1}), and $S_0 \rightarrow T_1$ (ΔE_{T1}) Transition Energies (in eV) and S_0 and S_1 Dipole Moments (μ_0 and μ_1 , in debye) for Acid and Base Forms of 2OH and Its Cyano Derivatives^a

molecule	acid					base					
	ΔE_1	ΔE_2	ΔE_{T1}	μ_0	μ_1	ΔE_1	ΔE_2	ΔE_{-1}	ΔE_{T1}	μ_0	μ_1
2OH	3.44	4.11	2.62	1.0 ^b	1.2 ^c	2.55	3.11	2.31	2.00	5.9	1.9 ^d
5CN	3.49	4.01	2.62	4.0 ^d	4.3 ^d	2.10	2.90	1.83	1.50	5.2	2.4 ^d
6CN	3.50	4.00	2.69	3.7	3.9	2.50	2.94	2.18	1.97	3.2	1.0
7CN	3.50	4.10	2.70	2.7	3.2	2.21	2.88	2.01	1.72	5.0	3.2
8CN	3.47	4.00	2.67	2.7	2.3	2.09	3.04	1.82	1.64	6.5	3.8
5,8DCN	3.34	3.80	2.51	0.7	2.0	1.90	2.98	1.68	1.32	5.4	1.3
6,8DCN	3.41	3.82	2.60	3.1	4.0	2.17	2.79	1.85	1.66	4.0	2.6

^a The dipole moments for the base form are calculated with the center of mass as the origin. Abbreviations: 2OH, 2-naphthol; *n*CN, *n*-cyano-2-naphthol; *n,m*DCN, *n,m*-dicyano-2-naphthol. ^b Estimated experimental value is 1.5 D (Table 43 of ref 41); CASSF gives 1.7 D (Table 5 of ref 38). ^c Estimated experimental value is 2.0 D (Table 8.1 of ref 7); CASSCF³⁸ gives 1.3 D. ^d Ab initio CASSCF calculations (Table 5 of ref 38) give $\mu_1 = 2.1$ D for 2OH anion, $\mu_0 = 3.5$ D, $\mu_1 = 3.6$ D for 5CN, and $\mu_1 = 4.3$ D for its anion.

The shift here is to the blue, commensurate with the larger negative charge on the oxygen in the GS. The sensitivity to α decreases significantly in the emission spectra as compared with the excitation spectra (see Figure 5 in ref 9), indicating a decrease in the ES charge density on the O⁻, rendering its HB stabilization less crucial. The importance of anion stabilization was also deduced from a study of ES proton transfer to methanol–water mixtures,³³ in which the decrease in the dissociation rate coefficient with increased methanol content was attributed to the diminishing ability of the lower dielectric solvent to solvate the anionic base.

Computational Methods

We have performed semiempirical computations on a series of gas-phase cyano-substituted 2-naphthols and their conjugate naphtholate bases. The AM1 calculations³⁴ using the AMPAC 6.55 package³⁵ included configuration interaction (CI, singly and multiply excited configurations between the eight highest occupied and eight lowest unoccupied orbitals).

As a first step, we have obtained the fully optimized ground-state geometries (without CI). Transition energies (vertical), dipole moments, and oscillator strengths were obtained by this method including CI. No solvent effects were incorporated in these calculations. We have found a negligible effect on the ES charge distribution upon geometry optimization (for example, the charge on the oxygen atom of excited 2OH increases by 0.005 electronic unit upon ES optimization). Therefore, the charge distribution (net charges) in S_1 of the acid form was calculated for the optimized ground-state geometry. S_1 geometries have been optimized for (unsubstituted) 2OH and for the anion form of all seven molecules, to allow the investigation of bond-length variations which occur upon excitation.

Results

Table 2 summarizes the calculated AM1 transition energies (ΔE) and (fixed) dipole moments (μ). Table 3 gives the Mulliken charge on the oxygen atom (q_O) of both acid and base in the first three singlet states. Table 4 compares it with experimental solvatochromic shift data, whereas Tables 5 and 6 depict the charges on the ring carbon atoms. The geometry is summarized in Tables 7–9. As a reference, Table 7 gives the CC bond lengths in naphthalene and its anion. Tables 8 and 9 provide a detailed description of the C–O and C–C bond lengths in the various electronic states of 2OH, its anion, and their cyano derivatives. The implications of these data are discussed below.

A. Transition Energies. Typically, S_1 is the third excited level for the acid (i.e., there are two lower-lying triplet states) and the second excited level for the base. The $S_0 - S_1$ transition

energies for the acid and base are given in Table 2. It is interesting to compare these values with experimental gas-phase data. Gas-phase 2OH has two rotamers, trans and cis, depending on the OH orientation with respect to the naphthalenic ring, their 0–0 transitions occurring in the absorption spectrum at 3.792 and 3.831 eV, respectively.^{36,37} From the R2PI spectrum of 5-cyano-2-naphthol (5CN), the values of 3.698 and 3.736 eV were obtained for the 0–0 transitions of the trans and cis rotamers, respectively.³⁸ We find vertical transition energies (ΔE_1) of 3.44 and 3.49 eV for 2OH and 5CN. Since the AM1 method is known to produce too small transition energies (up to ~ 1 eV), this agreement is actually quite good (even when the difference between adiabatic and vertical transitions is considered). However, the accuracy is not sufficient to mimic the shift between 2OH and 5CN.

The $S_0 - S_2$ transition energies (ΔE_2 , Table 2) are typically larger than ΔE_1 by ~ 0.5 eV. Thus (unlike the case of phenol¹⁰ or 1OH), we do not expect level crossing to occur for the 2OH derivatives.⁸ The transition dipole to S_2 is typically much larger than to S_1 (e.g., for 2OH: 0.040 vs 0.002 au, respectively).

The transition energies for the anions are considerably smaller than those of the acids, in line with the occurrence of ES proton transfer in these systems. Table 2 gives the transition energies (ΔE_{-1}) from the optimized S_1 state of the anions back to S_0 . These are compared with the experimental fluorescence frequencies in solution^{21,39} in Figure 1. First we note that the theoretical gas-phase transition energies are *smaller* than the experimental solution-phase values. This is not an error in the calculation: Due to the ICT effect, the solvent stabilizes the GS more than the ES. Such a solvent-induced blue-shift has been noted between the estimated gas-phase transition energy and the measured solution-phase absorption peak of phenol.¹⁰ Nevertheless, the substituent effects in the two phases are correlated, and this is corroborated by the figure. Hence the major effect of substitution on photoacidity must be related to the ICT effect even in solution.

- (33) Agmon, N.; Huppert, D.; Masad, A.; Pines, E. *J. Phys. Chem.* **1991**, *95*, 10407. Erratum, *J. Phys. Chem.* **1992**, *96*, 2020.
 (34) Dewar, M. J. S.; Zoeblich, E. G.; Healy, E. F.; Stewart, J. J. P. *J. Am. Chem. Soc.* **1985**, *107*, 3202.
 (35) Dewar, M. J. S.; Stewart, J. J. P.; Ruiz, J. M.; Liotard, D.; Healy, E. F.; Dennington II, R. D. *AMPAC Version 6.55*. Semichem., Shawnee, 1997–1999.
 (36) Oikawa, A.; Abe, H.; Mikami, N.; Ito, M. *J. Phys. Chem.* **1984**, *88*, 5180.
 (37) Johnson, M. J. R.; Jordan, K. D.; Plusquellic, D. F.; Pratt, D. W. *J. Chem. Phys.* **1990**, *93*, 2258.
 (38) Knochenmuss, R.; Sointsev, K. M.; Tolbert, L. M. *J. Phys. Chem. A* **2001**, *105*, 6393.
 (39) Soumillion, J. P.; Vandereecken, P.; Van Der Auweraer, M.; De Schryver, F. C.; Schanck, A. *J. Am. Chem. Soc.* **1989**, *111*, 2217.

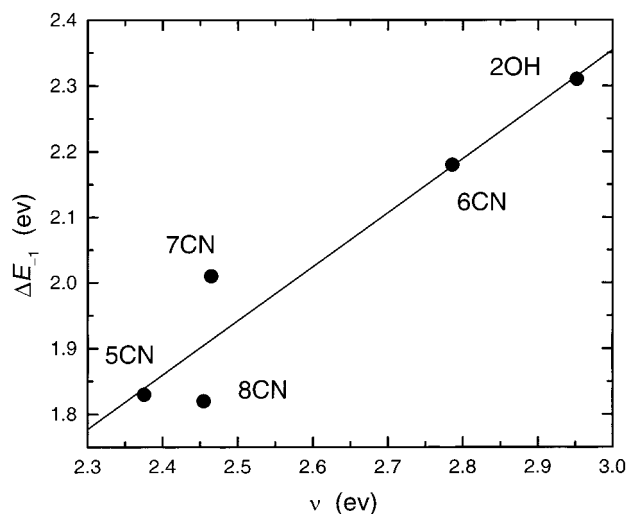


Figure 1. Correlation of the calculated (AM1) transition energies from the geometrically optimized S_1 state to S_0 , with the experimental fluorescence frequencies of 2-naphtholate³⁹ and its cyano derivatives²¹ in aqueous solutions.

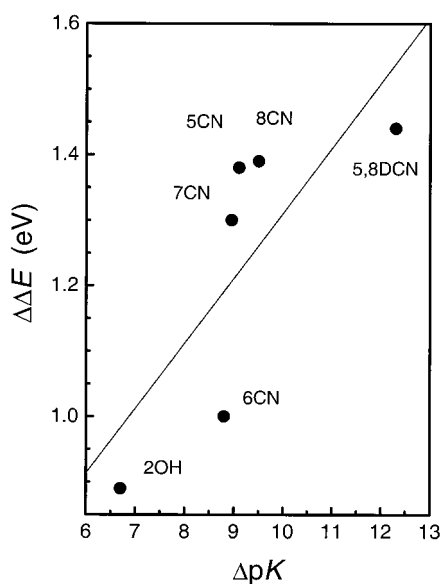


Figure 2. Correlation of the calculated (AM1) change in transition energies (Table 2) between acid and base with the experimental pK changes (Table 1)^{21–23} between the ground and excited state of cyano-2-naphthols in aqueous solutions. Chemical abbreviations are given in Table 2.

It is instructive to compare the difference in the calculated transition energies between acid and base, $\Delta\Delta E \equiv \Delta E_1(\text{ROH}) - \Delta E_1(\text{RO}^-)$, with the measured change in pK between the ground and excited state, $\Delta pK \equiv pK - pK^*$ (in aqueous solutions). On the basis of a thermodynamic cycle, equality is expected if all quantities refer to the same phase and one ignores zero-point energies (ZPE) and solvent relaxation. Gas-phase $\Delta\Delta E$ values (calculated here) are larger than the corresponding solution-phase values, because polar solvation diminishes $\Delta E_1(\text{ROH})$ and enhances $\Delta E_1(\text{RO}^-)$. Yet, a qualitative correlation exists between the two quantities, as shown in Figure 2. This correlation is, in fact, better than that found for ΔpK 's of cyanophenols using state-of-the-art CASSCF calculations with ZPE corrections and inclusion of solvent effects (Table 12 of ref 10). Possibly then, 2-naphthols are a better system for studying the origins of photoacidity.

Table 3. Mulliken Charge ($-q_O$) on the Hydroxyl Oxygen of the Acid and Base Forms of the Cyano-2-naphthols in Their First Three Singlet States^a

molecule	acid			base		
	S_0	S_1	S_2	S_0	S_1	S_2
2OH	0.246	0.208	0.209	0.504	0.374	0.426
5CN	0.242	0.204	0.216	0.473	0.363	0.411
6CN	0.243	0.195	0.188	0.466	0.384	0.402
7CN	0.243	0.198	0.210	0.473	0.365	0.407
8CN	0.243	0.198	0.202	0.462	0.369	0.416
5,8DCN	0.239	0.191	0.205	0.441	0.347	0.400
6,8DCN	0.240	0.195	0.186	0.435	0.361	0.398

^a See Table 2 for abbreviations.

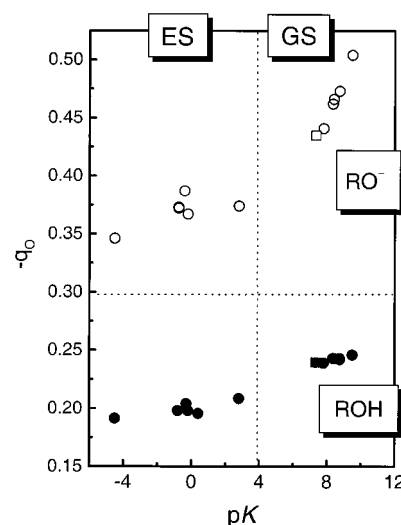


Figure 3. Correlation of acidity (Table 1)^{21–23} with the calculated net electron density on the oxygen atom (Table 3) for ground- and excited-state (S_1) cyanonaphthols in both their acid (full circles) and anion (open circles) forms. Squares are calculations for 6,8DCN, using a projected pK value of 7.35 (see Figure 4 below).

B. Electronic Charges. The dipole moment of a molecule gives an overall assessment for its intramolecular charge distribution. The calculated dipole moments for 2OH and its cyano derivatives are collected in Table 2. These are compared to experimental values and ab initio calculations, when available. They increase slightly with excitation for ROH (8CN is an exception) and decrease more dramatically with excitation for RO^- . This appears to be in line with the ICT effect, since the neutral ROH becomes more polar and the charged RO^- becomes less polar by the oxygen-to-ring charge transfer. The effect is larger for the anion, in line with the expectation for a greater importance of the ICT effect there.

Oxygen Charge. A more refined probe for the ICT effect is provided by the Mulliken charges on the various atoms. The electron donor is the oxygen atom, and its charge (q_O) is given in Table 3. Figure 3 shows that q_O for the six compounds correlates with the pK in both electronic states and for both acid and base. Again, experimental solution-phase data are compared here with calculated gas-phase charge densities. That equilibrium constants correlate with net electronic charges has recently been observed in another case, ground-state complexation of crown compounds with metal ions.⁴⁰

(40) Rurack, K.; Sczegan, M.; Spieles, M.; Resch-Genger, U.; Rettig, W. *Chem. Phys. Lett.* **2000**, *320*, 87.

(41) Minkin, V. I.; Osipov, O. A.; Zhdanov, Y. A. *Dipole Moments in Organic Chemistry*; Plenum: New York, 1970.

Table 4. Comparison between the Scaled Experimental Solvatochromic Slope Parameter, a ,⁹ and the Calculated Charge on the Oxygen Atom (Table 3, Using $q_H = 0.208$) in 2-Naphthol and Its Anion

	acid		base	
	S_0	S_1	S_0	S_1
a (cm ⁻¹)	270	0	3100	1770
$-(q_O + q_H)$	0.04	0	0.30	0.17
$0.3a/a_{\max}$	0.03	0	0.30	0.17

The ICT effect is seen in Figure 3 as a decrease in $|q_O|$ upon excitation. In agreement with the case of cyanophenols,¹⁰ the effect is rather small (yet nonvanishing) in the acid. It is considerably more dramatic for the anion, where q_O is more negative and $|q_O|$ decreases more drastically upon excitation.

This behavior may be compared quantitatively with the experimental solvatochromic study of 2OH by Solntsev et al.⁹ They considered the spectral shifts in the acid and base bands (the latter was investigated by Soumillion et al.³⁹) of 2OH for absorption (S_0 geometry) and emission (S_1 geometry). According to the Kamlet–Taft procedure,³² the frequency, ν , was fitted to

$$\nu = \nu_0 + p\pi^* + b\beta + a\alpha \quad (1)$$

where π^* , β , and α depict the polarity and hydrogen-bonding accepting and donating power of the solvent, respectively, in the Kamlet–Taft scale.³² The adjoint parameters p , b , and a represent *solute* properties. Let us focus on the parameter a , which reflects the negative charge on the oxygen to which the hydrogen bond is donated (the larger this charge, the larger is the stabilization effect of hydrogen bond donation). For the ROH form, Solntsev et al.⁹ performed this multilinear regression finding a small a parameter for the absorption spectrum (GS geometry) and a vanishing value for the emission spectrum (ES geometry). For the base (Figure 5 in ref 9), they found no dependence at all on π^* and β (i.e., $p = b = 0$), a very large a for the absorption spectrum, which decreased considerably for the emission spectrum. The corresponding values are summarized in Table 4.

The implications of these data, that ICT occurs in the ES to a small extent in the acid, and to a much larger extent in the

base form, can be confirmed quantitatively from our calculations by an appropriate scaling of the a parameter. Its minimal value, $a = 0$, occurs for the excited acid for which $q_O = -0.208$ (Table 3). From our calculations, the charge on the hydroxyl hydrogen is $q_H \approx 0.22$ in both electronic states. Thus, the total charge of the hydroxyl group for ROH(S_1) is indeed 0. Choosing $q_H = 0.208$, we add this value to q_O for all four states (second line in Table 4). The maximal value of a occurs for the GS base, RO⁻ (S_0), where $a = a_{\max} = 3100$ cm⁻¹ and $|q_O + q_H| = 0.30$. Scaling a by the ratio of these two quantities, we obtain the last line in Table 4, which is in excellent agreement with the OH charges for the two remaining cases, ROH(S_0) and RO⁻(S_1).

Ring Charges. We continue by considering the charges on the ring carbons for 2OH and its anion in their first three singlet states, Table 5. All the carbon atoms are electronegative, except for C₂, which bears a positive charge. The table can be used to identify the sites to which the charge migrates, predominantly for the anion. It is seen that, in the GS of 2-naphtholate, excess electronic charge is found in positions 1, 3, 6, 8, and (to a lesser extent) on carbon 10, in agreement with the resonance structures in Chart 2. (Note: the charge on the CH hydrogen is about +0.1.) The largest negative charge resides at position 1, in agreement with the observation that thermal H/D exchange in 2OH occurs at this position.¹⁴

Upon excitation to S_1 , $-q_{C_i}$ increases for $i = 3, 5$, and 8 and decreases on carbons 1 and 6. These findings are in agreement with the observation²³ that, of the four monocyno derivatives synthesized (5CN, 6CN, 7CN, 8CN), 6CN and 8CN are the most acidic in the GS, whereas 5CN and 8CN are the most acidic in the ES (Table I). It is not clear whether the simplistic valence bond arguments could explain this observation, since there is no resonance structure with excess charge on C₅.

Table 6 shows that this effect is even more pronounced for the cyano derivatives. Exceptional are those sites to which CN substituents are bound. Their electronic charge is reduced by ICT to the CN moiety. Hitherto unexpected is the role of the proximal ring in solvating the charge. As resonance structures c and d of Chart 2 suggest, and our calculation corroborate, the charge does not migrate exclusively to the distal ring. Rather,

Table 5. Mulliken Charges (q_{C_i}) on the Ring Carbon Atoms of 2OH (above Line) and Its Anion (below Line) in the First Three Singlet States^a

state	C ₁	C ₂	C ₃	C ₄	C ₅	C ₆	C ₇	C ₈	C ₉	C ₁₀
S_0	-0.207	0.071	-0.131	-0.102	-0.112	-0.135	-0.122	-0.123	-0.010	-0.052
S_1	-0.179	0.041	-0.168	-0.090	-0.109	-0.121	-0.131	-0.110	-0.031	-0.061
S_2	-0.244	0.188	-0.180	-0.100	-0.056	-0.196	-0.082	-0.127	-0.021	-0.077
S_0	-0.346	0.258	-0.234	-0.111	-0.091	-0.229	-0.136	-0.173	0.039	-0.146
S_1	-0.148	0.259	-0.373	-0.058	-0.296	-0.125	-0.183	-0.319	-0.001	-0.063
S_2	-0.181	0.195	-0.219	-0.124	-0.135	-0.295	-0.219	-0.133	-0.086	-0.075

^a From geometry-optimized AM1 calculations with a 16-orbital active-space CI.

Table 6. Mulliken Charges ($-q_{C_i}$) on Select Ring Carbon Atoms of Cyanonaphtholates (the Anion Form) in the Ground/Excited State^a

molecule	C ₁	C ₃	C ₅	C ₆	C ₈
5CN	0.334/0.080	0.235/0.334	-0.003/0.177	0.192/0.134	0.147/0.315
6CN	0.335/0.097	0.237/0.365	0.048/0.276	0.155/0.078	0.174/0.290
7CN	0.335/0.121	0.238/0.331	0.088/0.242	0.209/0.059	0.119/0.317
8CN	0.343/0.081	0.239/0.351	0.079/0.255	0.244/0.125	0.089/0.199
5,8DCN	0.343/0.068	0.224/0.354	-0.018/0.125	0.204/0.090	0.081/0.204
6,8DCN	0.322/0.067	0.233/0.349	0.029/0.230	0.163/0.029	0.093/0.192

^a Note how the electronic charge decreases, upon excitation, on carbons 1 and 6, whereas it increases on carbons 3, 5, and 8.

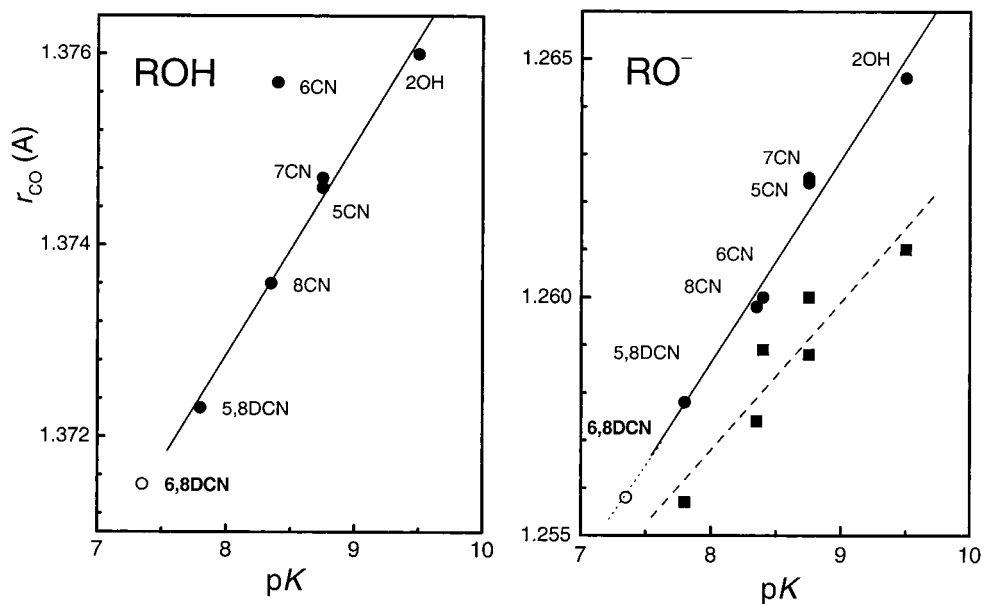


Figure 4. Correlation of the calculated (AM1) C–O bond length (Table 9) with experimental pK values (Table 1) for ground-state acid and base forms of cyano-2-naphthols (filled circles). The prediction for the yet unsynthesized 6,8DCN dye is shown as an open circle. For the anion form, the bond lengths in S_1 are shown as squares.

Table 7. Calculated Carbon–Carbon Bond Lengths (in Å) for Naphthalene and Its Anion in Their (Optimized) Ground State

molecule	9–1	1–2	2–3	9–10
naphthalene (AM1)	1.422	1.373	1.416	1.419
(HF/6-31G) ¹⁹	1.420	1.362	1.416	1.413
naphthalene anion (AM1)	1.410	1.398	1.387	1.441

a sizable fraction resides on the proximal ring, predominantly in the ES, where C_3 becomes the most negatively charged atom.

C. Geometry. Variations in bond lengths of 2OH, its anion, and their derivatives can be better appreciated in comparison with the geometry of naphthalene and its anion (Table 7). Naphthalene (D_{2h} symmetry) assumes an alternate structure, with a long C_9 – C_1 bond and a short C_1 – C_2 bond, but this alternation is not uniform (the C_9 – C_{10} and C_2 – C_3 bonds have almost equal lengths). Similar results have been obtained by ab initio calculations;¹⁹ see Table 7. In the anion, the peripheral bonds equalize whereas the central, C_9 – C_{10} , bond lengthens. In terms of the three valence bond (VB) resonance structures for naphthalene, it thus appears that the contribution of the structure with a central (9–10) double bond diminishes in the anionic form.

The geometry of 2OH is given in Table 8. Its GS is similar to that of naphthalene (Table 7). The insertion of the hydroxyl causes the two adjacent CC bonds to lengthen, but the other CC bonds (particularly in the distal ring) are nearly unchanged. In contrast, the anions behave differently: Whereas the naphthalene anion (Table 7) has more uniform bond lengths,

naphtholate (Table 8) shows enhanced bond-length alternation, with C_3 – C_4 and C_9 – C_1 being the shortest CC bonds in the proximal ring, and with C_5 – C_6 and C_7 – C_8 the shortest bonds in the distal ring. In terms of resonance structures, this bonding pattern resembles most closely structure e, in contrast to the charge distribution which is a mixture of all resonance structures, a–e, in Chart 2.

The C–C bonds in the anion tend to equalize in S_1 ; the longer ones shorten and the short ones lengthen. The ES bonding pattern does not seem to lend itself to a simple interpretation in terms of VB structures.

Moving on to the substituent effect, we note that several bond lengths correlate with the pK (Table 9). The best correlation appears to hold with the C–O bond lengths in the GS, which are around 1.37 Å in the acid, shortening to 1.26 Å in the anion. With increasing GS acidity, the C–O bonds in both forms shorten (Figure 4). The correlation shown is quite remarkable, allowing us to predict, by extrapolation, that the pK of the yet to be synthesized 6,8-dicyano derivative should be 7.35. The figure also shows that, upon excitation of the anionic derivatives (to S_1), this bond further shortens, and this again agrees with the ICT effect, which is expected to play a dominant role in anion stabilization. Figure 5 shows that other bonds in the proximal ring of the GS anions also correlate with the pK . Typically we observe that, with increasing acidity, the short bonds shorten even further, whereas the long ones lengthen further.

Table 8. Calculated (AM1, Optimized Geometries) Carbon–Carbon Bond Lengths (in Å) for 2OH (above Line) and Its Anion (below Line) in Its First Three Singlet States

state	9–1	1–2	2–3	3–4	4–10	10–5	5–6	6–7	7–8	8–9	9–10
S_0	1.4197	1.3806	1.4260	1.3697	1.4235	1.4207	1.3737	1.4154	1.3734	1.4221	1.4188
S_1	1.3978	1.4188	1.4234	1.3996	1.4063	1.4041	1.3928	1.4085	1.3911	1.4017	1.4690
S_2	1.3944	1.4250	1.4052	1.3901	1.4190	1.3969	1.4067	1.3944	1.3941	1.4154	1.4545
S_0	1.3897	1.4299	1.4615	1.3589	1.4257	1.4082	1.3786	1.4257	1.3703	1.4325	1.4324
S_1	1.4119	1.4120	1.4533	1.3737	1.4173	1.4201	1.4024	1.3840	1.4076	1.4014	1.3804
S_2	1.4195	1.4461	1.4487	1.3672	1.4240	1.3973	1.3934	1.4150	1.3940	1.4063	1.4501

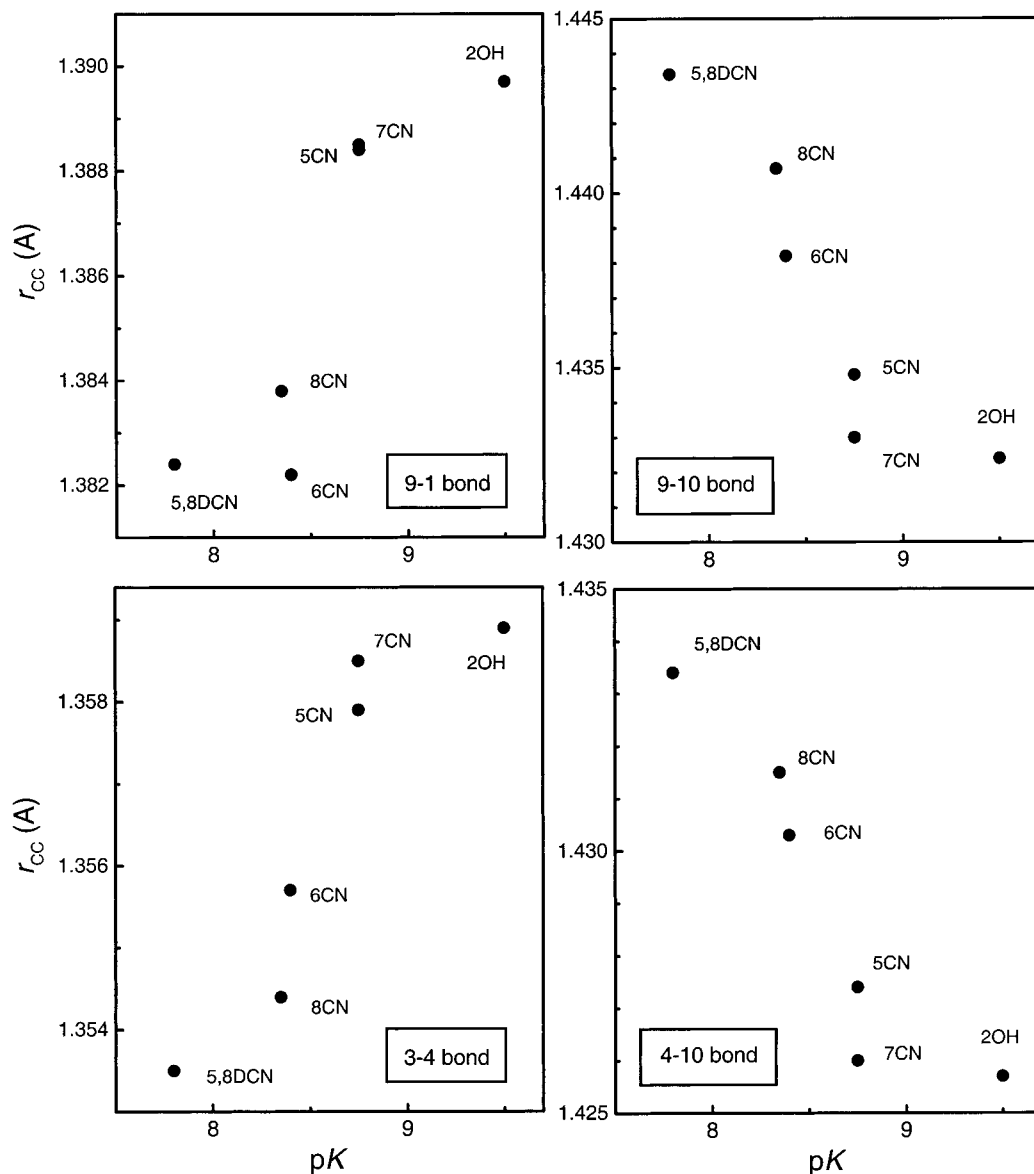


Figure 5. Correlation of four calculated ring C–C bond lengths with experimental pK values for ground-state cyano-2-naphtholates.

Table 9. Calculated (AM1, Optimized Geometries) Bond Lengths (in Å) for Cyano-Substituted 2-Naphtholates (Anion Form) in Their Ground/Excited States^a

molecule	C ₂ –O	C ₉ –C ₁	C ₁ –C ₂	C ₂ –C ₃	C ₃ –C ₄	C ₄ –C ₁₀	C ₁₀ –C ₉
2OH	1.265/1.261	1.390/1.412	1.430/1.412	1.461/1.453	1.359/1.374	1.426/1.417	1.432/1.380
5CN	1.262/1.260	1.388/1.416	1.431/1.449	1.462/1.450	1.358/1.364	1.427/1.421	1.435/1.421
6CN	1.260/1.259	1.382/1.409	1.436/1.455	1.464/1.442	1.356/1.375	1.430/1.416	1.438/1.429
7CN	1.262/1.259	1.388/1.412	1.432/1.446	1.462/1.455	1.358/1.362	1.426/1.421	1.433/1.430
8CN	1.260/1.257	1.384/1.409	1.434/1.455	1.465/1.448	1.354/1.366	1.431/1.419	1.441/1.430
5,8DCN	1.258/1.256	1.382/1.418	1.435/1.458	1.466/1.449	1.353/1.365	1.433/1.422	1.443/1.424
6,8DCN	1.256/1.255	1.377/1.413	1.440/1.457	1.467/1.447	1.352/1.367	1.435/1.419	1.445/1.422

^a See Table 2 for abbreviations.

Discussion

We believe this computational work provides convincing evidence that intramolecular charge migration from the hydroxyl oxygen to the aromatic ring does occur upon excitation of 2-naphthol and its cyano derivatives and that the dominance of this effect for the *anion*^{8–10} plays a major role in promoting photoacidity. The question arises, what is the electronic mechanism leading to this effect? One may try to address this question using molecular orbital or valence bond terminology.

A. Molecular Orbitals: The Concept of Antiaromaticity.

The systematic geometrical changes between S_0 and S_1 hint that the effect has a common origin with the aromaticity of cyclic conjugated π systems.¹⁶ As first suggested by Hückel, carbocyclic molecules with $4n + 2\pi$ electrons (n integer) have an aromatic character, stabilizing them by electronic delocalization around the ring.²⁰ In contrast, systems with $4n$ conjugated π electrons are antiaromatic. Their destabilization results in geometric perturbations with alternating short and long bonds

in the ring. In addition to bond alternation, antiaromatic molecules are often characterized by a small singlet–triplet ($S_0 - T_1$) gap (ΔE_{T1}), sometimes as small as 0.5 eV (as opposed to ~ 3 eV in aromatic molecules).²⁰ A classic example is cyclobutadiene, which possesses two single and two double bonds. It is known for thirty years that Hückel's rules are reversed in the triplet states, so that in T_1 cyclobutadiene becomes a symmetric, aromatic molecule.¹⁷ More recently, it was realized that cyclobutadiene becomes a symmetric square also in the S_1 state.¹⁸ In fact, in the excited singlet state, the bond lengths tend to equalize for both aromatic and antiaromatic molecules.¹⁹ Naphthalene is an aromatic molecule, possessing 10 π electrons ($n = 2$). The 2-naphthol derivatives are also aromatic, as judged from the rather large (and nearly substituent independent) singlet–triplet gap (Table 2) as well as from their geometry, which resembles that of naphthalene. However, in the anion form, conjugation of the oxygen charge into the aromatic ring would lead to a 12-electron system that should possess some antiaromatic character. As opposed to the decrease in bond-length alternation in the naphthalene anion, in naphtholate, we find a shortening of the CO bond and *enhanced* bond-length alternation within the ring. This is also corroborated by the ΔE_{T1} values in Table 2, which are smaller than for the acid and decrease even further with the electron-withdrawing cyano substitution. For example, in 5,8-DCN (the most acidic derivative yet synthesized), ΔE_{T1} drops from 2.5 to 1.3 eV. Since the decrease in the $S_0 - S_1$ gap parallels that of the $S_0 - T_1$ gap, decrease in aromaticity of the anion form parallels the increase in acidity.

Thus, in the GS of the anion, there are two opposing effects: increasing delocalization of the oxygen charge, coupled to a decrease in the aromatic character of the ring system. In S_1 , we find a more tempered variation in the alternating bond-lengths pattern, suggesting an increase in the aromatic character. The more symmetric ring system in the ES is better for delocalizing the excess electron(s) originating from the hydroxyl oxygen, and this could be the origin of the photoacidity phenomenon.

B. Valence Bond: New Synthetic Candidates? Using VB terminology, we may consider the electronic state to be a mixture of the five ionic resonance structures depicted in Chart 2. Starting from C_2 , these structures locate the negative charge on every second carbon atom (clockwise: 3, 10, 6, 8, and 1). Indeed, for the GS of the anion, these appear to be the most electron-rich sites along the aromatic skeleton. In the ES state, we observe that the electronic charge in positions 1, 6, and 10 diminishes, whereas it grows in positions 3, 5, and 8. Since there is no resonance structure with the charge localized in position 5, the ES charge density cannot be as easily rationalized by such VB terminology.

The Mulliken charges on the naphtholate ring system bear a close relationship with the acidity of the corresponding cyano-

substituted compounds. In the synthetic work done thus far, CN substituents were placed at different positions in the distal ring.^{21,22} It was found that in the GS the 6- and 8-substitutions lead to lower pK' 's, whereas in S_1 the 5- and 8-substitutions lead to lower pK^{*} 's. These indeed correspond to the most electron-rich sites on the distal ring according to our AM1 calculations for S_0 and S_1 . Hence, placing an electron-withdrawing substituent on the more electronegative sites of the 2OH anion appears to enhance the acidity.

Since cyano substitution on the proximal ring has not yet been attempted,^{21,22} it may be interesting to check whether the same principle holds there also. According to our calculations, 1-cyano-2-naphthol (1CN) should be a slightly stronger acid in its GS, and more interesting, 3-cyano-2-naphthol (3CN) should be a strong photoacid, as suggested by the enhanced negative charge in position 3 of excited 2OH. (It corresponds to resonance structure d in Chart 2, the only one *without* a 3–4 double bond). Subsequently, 3,5,8-tricyano-2-naphthol might be the ultimate superphotoacid from this family. If such logic is found to be generally valid, it could provide a useful tool for selecting favorable synthetic candidates for the preparation of new “super”photoacids.

Summary

We have reported systematic semiempirical quantum calculations for 2-naphthol and some of its cyano derivatives in both ground and excited states and for both neutral and anionic forms. From an investigation of the variation in charge distribution and bond lengths, several tentative conclusions were drawn:

Intramolecular charge transfer from the hydroxyl to the aromatic system occurs upon excitation, but it is considerably more pronounced for the anion form than for the neutral photoacid.

The ICT effect reduces the aromatic character of the anion in its ground state much more than in its excited S_1 state, and as a result, the $S_0 - S_1$ gap decreases and with it the photoacidity increases.

Systematic variations in charge density and bond lengths are observed within this cyanonaphthol family. The more acidic compounds exhibit a smaller negative charge on the oxygen and a shorter CO bond length.

Substitution in the more electronegative ring sites leads to more acidic compounds.

Acknowledgment. We thank Z. R. Grabowski, D. Huppert, J. T. Hynes, S. Shaik, K. M. Solntsev, W. Thiel, and J. Waluk for inspiring correspondence and discussions. This work was supported in part by a grant from the U.S.–Israel Binational Science Foundation.

JA003875M